

A prototype synthesis and characterization of hydroxyapatite bioceramics nanocrystallites

Pramod N. Jagadale^{1*}, Pramod P. Jagtap², Meghnad G. Joshi³, Sambhaji R. Bamane⁴

¹Department of Chemistry, Y. M. College, Bharati Vidyapeeth Deemed University, Pune 411038, Maharashtra, India

²Metal Oxide Research Laboratory, Department of Chemistry, Dr. Patangrao Kadam Mahavidyalaya, Sangli 416416, Maharashtra, India

³Stem Plus Biotech Pvt. Ltd, Block-11, Shiv Meridian, M G Road, Sangli 416416, Maharashtra, India

⁴Raja Shripatrao Bhagwantrao Mahavidyalaya, Aundh, Dist-Satara, Maharashtra, India

*Corresponding author. E-mail: pramodbioceramics@gmail.com

Received: 07 February 2015, Revised: 27 November 2015 and Accepted: 30 January 2016

ABSTRACT

Novel porous bioactive hydroxyapatite (HAP) nanocrystallites were synthesized by auto-combustion technique. The texture properties of the HAP nanopowder were determined through series of characterization techniques. The thermal decomposition behaviour and required sintering temperature of citrate precursor to phase formation of the sample was checked by thermogravimetric analysis (TG-DTA). The hexagonal structure and porous nature of the material were estimated by using X-ray diffraction (XRD) and electron microscopy scanned with different magnifications. Phase formation of HAP was determined by FTIR technique. Transmission electron microscopic (TEM) study indicated the nanostructure of the ceramics, particle size was found to be 30 - 35 nm. These nanoparticles were evaluated for the qualitative and quantitative determination of different elements by energy-dispersive X-ray spectroscopy. In vitro MTT assays showed HAP nanopowder have good biocompatibility and promotes cell proliferation. This nanostructured HAP powder with enhanced biocompatibility can be potentially used as a material for bone tissue engineering. Copyright © 2016 VBRI Press.

Keywords: Nanocrystallites; hydroxyapatite; porous material; MTT assays.

Introduction

Biomaterials especially the inorganic, calcium phosphate the one among many does have the extensive applications in medicinal sector [1, 2]. Currently, hydroxyapatite (HAP, $\text{Ca}_{10}(\text{PO}_4)_6(\text{OH})_2$) is an example of promising ceramic biomaterial because of its bioactivity, nontoxic, and non-inflammatory properties [3, 4]. Sinterability, solubility, fracture toughness, castability and absorption are the basic physical properties of HAP. Controlled and calculative tailoring of particle size, morphology along with help of different physical parameters, these can be adapted in various fields [5, 6].

Reporting important advantages of the synthetic HAP, they offer good osteoconductive and osteoinductive capabilities [7, 8]. Taniguchi *et al.* [9] through the investigations sintered HAP exhibited outstanding biocompatibility with soft tissue like muscles and gums. The mentioned potential of the HAP has made it as supreme contender for orthopaedic and dental implants. Concerning the hard tissues mostly the synthetic HAP has its extensive usage especially for the repair and then on for general usage is the coating of implants, bone augmentation and bone repair also it acts as fillers in bone or teeth [10, 11]. All the discussed applications and the characters it seems to give great importance and a special significance to devise method for the synthesis of HAP that can have precise control over particle size and morphology.

Different synthetic strategies have been explored for the process of synthesizing HAP. This include ultrasound assisted method [12], freezing organic-inorganic soft

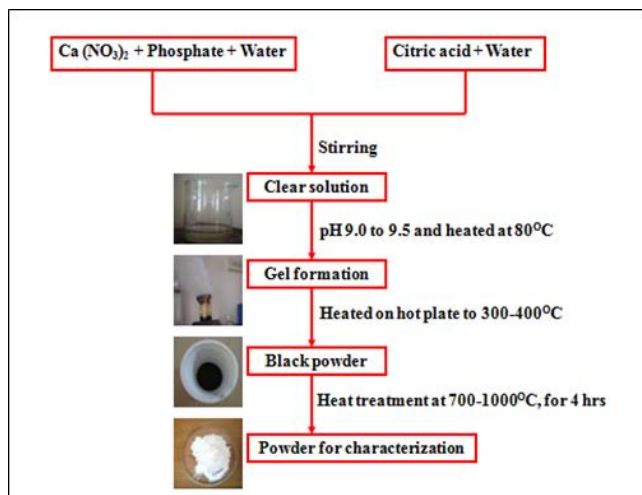
solution [13], co-precipitation method [14], microwave hydrothermal method [15], mechanochemical method [16], sol-gel method [17] and microemulsion route, [18]. From the above read list, considering the size confinement and creating porosity both, auto-combustion method is judged as the best. Auto-combustion method with citric acid enacting as fuel is a simplistic one-pot way to acquire HAP nanoparticles with pure phase and high crystalline.

However, new techniques for expanding bone tissue engineering field consist of the use of mesenchymal stem cells (MMSc) isolated from bone marrow [19]. In this context, paper aims to synthesis nanocrystalline hydroxyapatite through a simple and low cost auto-combustion method using citric acid as fuel. The materials obtained were characterized by TG-DTA, XRD, FTIR, SEM, EDAX, and TEM to explore their structural properties.

Experimental and material details

Nanostructured HAP sample having general formula $\text{Ca}_{10}(\text{PO}_4)_6(\text{OH})_2$ was synthesized by auto-combustion method. The combustion synthesis was carried out with the calcium nitrate, diammonium hydrogen phosphate and citric acid were used as sources of Ca, P and fuel respectively. All chemical used in synthesis are of analytical Grade. The molar ratio of both metal nitrate and phosphate to citric acid was taken as 1:2. Firstly, stoichiometric amount calcium nitrate and diammonium hydrogen phosphate were dissolved in millipore water with vigorous stirring. Citric acid was weighted

stoichiometrically and dissolved in distilled water. The above solution mixed under constant stirring and pH adjusted 9 to 9.5 using ammonia. A homogeneous clear solution was achieved. A homogeneous clear solution was achieved. This clear solution was stirred vigorously and heated up to 80 °C for 4 h to obtain gel. Further, dry HAP powder was obtained by heating of gel at 300 - 400 °C. This dried HAP was further sintered at 700-1000 °C for 4 h and used for further characterization (**Scheme 1**).



Scheme 1. HAP bioceramics synthesis by auto-combustion technique.

Materials characterization

The thermal decomposition behaviour and required sintering temperature of citrate precursor to phase formation of the sample was checked by thermogravimetric analysis on the SDT Q-600 instrument by heating the powder after auto-combustion in air atmosphere from 20 to 1000 °C at the rate of 10 °C per min. The X-ray diffraction analysis was used to know phase purity of synthesized material by using PW3710 (Model- Philips) with CuK α radiation ($\lambda = 1.5406\text{\AA}$). Morphology of synthesized HAP sample was studied by TEM analysis (Philips CM-200) at 200 kV. The surface topography and microstructure of the sample was examined by means of electron microscopy scanned with different magnifications (JEOL JSM-6360). These nanoparticles were evaluated for the qualitative and quantitative determination of different elements by energy-dispersive X-ray spectroscopy (JEOL JSM-6360). JASCO FT/IR-6100 type 'A' spectrometer was used for FTIR study of these nanoparticles.

Cell culture experiments

To study the biocompatibility of HAP, an in vitro test was performed. The human bone marrow mesenchymal stem cells (BMMSCs) and cord blood mesenchymal stem cells (CBMSCs) from a passage 4-6 were used and cultured using the method described by earlier [20]. Prior to bioceramics surface cell seeding, cells were revived and cultured in Dulbecco's minimum essential medium (DMEM, Make-Sigma Aldrich) with fetal bovine serum (FBS) 10 %, 1mM sodium pyruvate, 2mM L-glutamine, streptomycin (50 mg/mL) and penicillin (50 U/mL) as a

supplement. The concentration of 5×10^5 cells per well were used for seeding in 6-well plates with 2 mL of DMEM. Further, incubation of the cells was done for growth and proliferation in CO₂ incubator optimized at 5 % CO₂, 90 % humidity with temperature at 37°C. The cells were cultured with 20, 60, and 80 μg HAP/ml for 12, 24 and 48 hours (70 % confluency) before the assays.

MTT cytotoxicity test

MTT cytotoxicity test is very important to evaluate cell viability and cell proliferation of bioceramic materials. As synthesized HAP sample was therefore analyzed by MTT cytotoxicity test to study cell cytotoxicity, proliferation and viability. Well-characterized BMMSCs and CBMSCs cells were used and cultured by culture method described previously. Each composition was taken in three replicate. Initially, autoclaved samples were positioned in the well plate and consequently washed with PBS. After that, 96 well plates were seeded with concentration of 5×10^5 cells per mL. Afterward, the incubation of culture plate in CO₂ incubator was done for 12, 24 and 48 hours. Subsequently, the medium was aspirated and then samples were washed with PBS twice. 20 μL of MTT dye solution [(3-(4, 5-dimethylthiazol-2-yl) -2, 5 diphenyltetrazolium bromide: Make-SIGMA, USA, Cat no.M5655)] and 5 mg per mL phosphate buffer was added to each well so as to pH =7.4. Lastly, the incubation of plate for 15 min and 4 h was done for steady-state confluent cells and exponentially growing cells respectively. After the incubation, the samples were taken off from the well and the crystals were solubilized with help of DMSO (200 μL) and this solution was energetically stirred for dissolution of the reacted dye. ELISA automated microplate reader was used to check the absorbance of each well at 550 nm (Biorad). All data were given in form of mean \pm SD for three group samples. The culture medium without cells is used as blank to calibrate the spectrophotometer at zero.

The viability of the cell in percentage is related to control wells containing cell culture medium without any addition of nanoparticles and was analyzed using the formula:

$$\text{Cell viabilities (\%)} = [A] / [AB] \times 100 \quad (1)$$

where, A and [AB] is the absorbance of the test sample and control sample respectively.

Results and discussion

TGA-DTA analysis

Thermal stability of HAP ceramic sample was examined by thermal decomposition of the powder. The TGA-DTA results as shown in **Fig. 1**, it was observed that decomposition of HAP sample below 200 °C due to removal of absorbed water. Decomposition during 200–320 °C can be mainly due to degradation of organic residual part. DTA curve shows that thermal decomposition of HAP sample at 100 °C, 200 °C and 250 °C with an endothermic peak and this peak is only due to degradation of residual water from gel. TGA shows weight loss in the

temperature range of 100-200 °C indicated the reactions (oxidation-reduction) of nitrates with fuel [21].

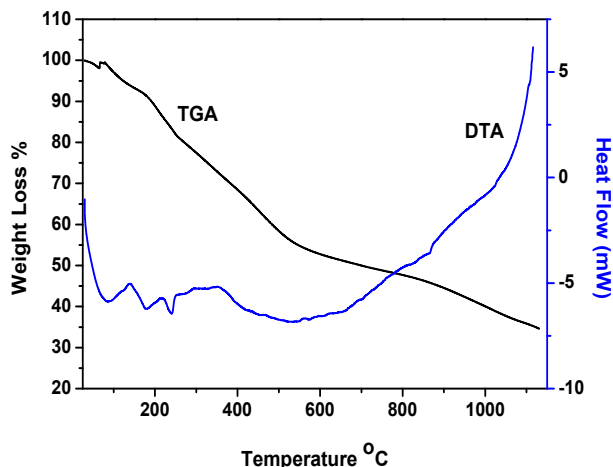


Fig. 1. TGA-DTA curve of HAP as synthesized powder.

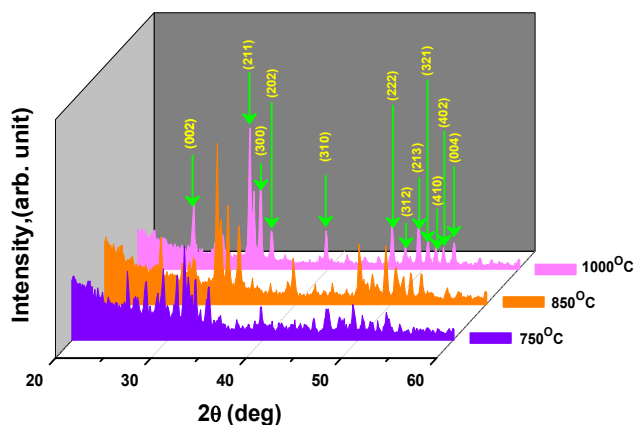


Fig. 2. XRD patterns for HAP samples: (a) calcined at 750 °C, (b) calcined at 850 °C, (c) calcined at 1000 °C.

XRD analysis

The X-ray diffraction study was carried out on HAP prepared by auto-combustion method annealed at various temperatures is shown in **Fig. 2**. The XRD analysis of these samples exhibit almost similar patterns with each other except changes in peak height and peak width with increases in temperature. This pattern corresponds to peaks of (002), (211), (300), (202), (310), (311), (113), (222), (312), (213), (321), (410), (402) and (004). These polycrystalline HAP nanoparticles exhibit single phase hexagonal structure with no additional peaks (JCPDS 09-0432) [22]. Lattice parameters of HAP was found to be $a = 9.418 \text{ \AA}$ and $c = 6.881 \text{ \AA}$. The average crystallite size of synthesized HAP sample was estimated by using Debye Scherrer's formula [23-25].

$$\tau = 0.94 * \lambda / \beta * \cos \theta \quad (2)$$

where, crystallite size (τ) depends upon wavelength λ (1.54 Å for CuK α) of the X- ray and the FWHM (β) of the XRD peak at 2θ . The average crystallite size obtained for HAP sample calcined at 1000°C was found to be ~ 30 nm.

FTIR analysis

A representative FTIR spectrum of the HAP nanoparticles prepared by auto-combustion method presented in **Fig. 3** and found to be very similar to those observed by D. Gopi and V. Stanic *et al.* [26,27]. The peak located approximately at 3571 cm^{-1} and 632 cm^{-1} corresponds to stretching mode and vibrational mode of the OH⁻ group. The strong doublet band (shoulder band) at 960-1100 cm^{-1} was assigned to the P-O stretching vibration of the phosphate group (PO₄³⁻). The weak band for phosphate bending vibration appears at 473 cm^{-1} . Moreover, the doublet band at 570-601 cm^{-1} was assigned to the PO₄³⁻ bending mode. A small band at around 1650 cm^{-1} was possibly due to absorbed water. The FTIR result demonstrates that the synthesized HAP sample was in high purity state [26].

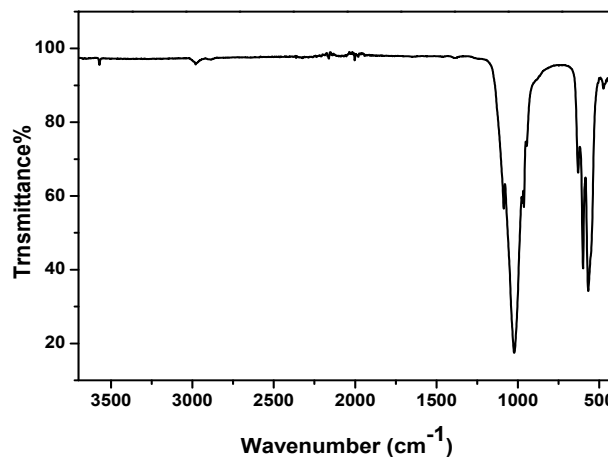


Fig. 3. FT-IR spectrum for nanoHAP sintered at 1000 °C.

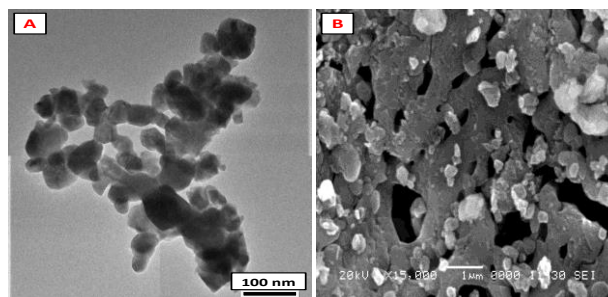


Fig. 4. TEM (a) and SEM (b) micrographs of HAP sintered at 1000 °C.

TEM and SEM analysis

Transmission electron microscopy (TEM) can provide very useful information about shape and size of the particle. **Fig. 4(A)** shows the TEM micrograph of nanohydroxyapatite calcined at 1000 °C in air for 4 h. From the micrograph it is observed that the nanoparticles have spherical shape and well dispersed without evident aggregation. The images suggest that the particle size of around 30-35 nm and this value is in the close vicinity to value obtained from XRD analysis.

SEM instrument have been invoked to know the morphology of the obtained HAP. **Fig. 4(B)** shows the SEM images of HAP particles and reveals that as prepared HAP product consist of many pores having irregular shape

with separated with infinitesimal distance. The formation of pores is beneficial, and finds very useful applications in drug carriers [28] and bone tissue engineering as they would permit the cell adhesion and proliferation [29].

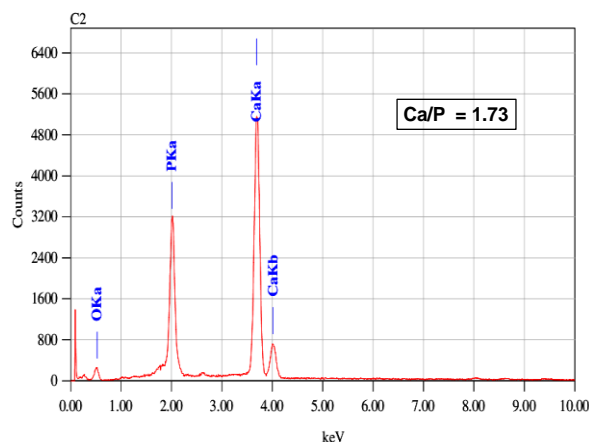


Fig. 5. Energy dispersive spectra of HAP.

EDAX analysis

The elemental composition and homogeneity of particles have significant effects on biocompatibility and bioactivity properties of bioceramic materials. To understand interrelationship between materials properties, composition of the material must be known. This technique was used to analyze HAP sample. An EDAX spectrum of this sample is shown in Fig. 5. Biological reactions of a HAP samples are strongly dependent on its chemical composition, i.e., Ca/P ratios; human bone primarily consists of Ca and P with a Ca/P ratio from 1.4 to 1.7 [30]. EDAX result reveals that HAP sample contains Ca, P and O without any impurity. The optimum Ca/P ratio for synthesized sample was found to be 1.73, which is slightly greater than 1.67 (theoretical value) and the same was commonly reported [31].

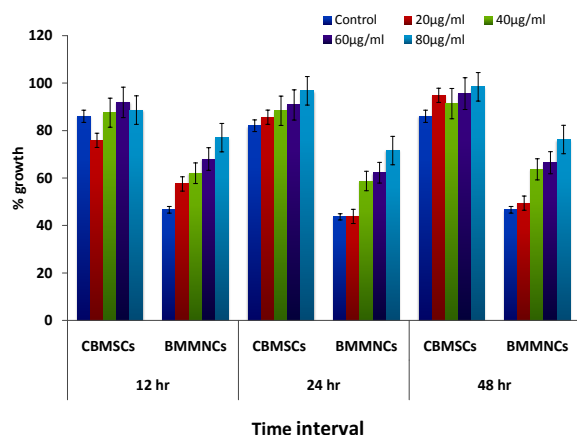


Fig. 6. MTT assay results showing the BMMSCs and CBMSCs proliferation on HAP sample after 12, 24 and 48 h of culturing.

Cell growth measurement

MTT assay test were used to evaluate cell proliferation, cell viability of synthesized HAP sample that helps to develop new biomedical applications and the result is predicted in Fig. 6. Mesenchymal stem cells (MSCs) can be

distinguished into cell type multiplicity and extensively used in tissue engineering. In present investigation, to evaluate in vitro cytotoxicity, tissue culture plates were used as a reference, and it is compared with synthesized HAP nanopowders by using BMMSCs and CBMSCs cells. From the results it is seen that growth rate of cell viability for both the cells are depend upon incubation period and concentration of HAP nanopowder. When the concentration of HAP nanopowder was 80 μg/mL and incubation period was 48 h, the value of cell viability for CBMSCs cells was 98.42 %. However, after 12 and 24 h there is slight decreases in percentage viability of CBMSCs, although it is not statistically significant compared to control. While, BMMSCs showed 70-77 ± 4.95 % viability compared to control. Percentage viability in BMMSCs after 48 h and 12 h was similar. This result was therefore found to be suitable for good biocompatibility of HAP nanoparticles for all concentrations. The results were formulated as mean standard deviation (SD) and this result was established at a level of $p < 0.05$.

Conclusion

- Hydroxyapatite (HAP) nanoparticles with improved and unique applications in tissue engineering were synthesized by innovative auto-combustion synthesis route.
- Crystallite size obtained from XRD was found to be 30 nm.
- The elemental analysis and presence of different elements such as Ca, P and O without any impurity for synthesized nanomaterials was confirmed by EDAX.
- Particle size obtained from TEM analysis was found to be good agreement with the value obtained from XRD pattern.
- Cell culture, MTT and cell adhesion assay showed that the nanosized HAP powder provided a more adequate environment for cell adhesion and proliferation and was characterized by good biocompatibility.

Acknowledgements

The author would like to express their thanks to UGC, New Delhi for financial support through Major Research Project [F.No.34-296/2008 (SR)].

Reference

1. Vallet-Regi, M.; González-Calbet, J. M., *Solid State Chem.* **2004**, *32*, 1.
DOI: [10.1016/j.progsolidstchem.2004.07.001](https://doi.org/10.1016/j.progsolidstchem.2004.07.001)
2. Dorozhkin, S.V., *Materials*, **2009**, *2*, 1975.
DOI: [10.3390/ma2041975](https://doi.org/10.3390/ma2041975)
3. Cai, Y.R.; Tang, R. K.; *J Mater Chem.* **2008**, *18*, 3775.
DOI: [10.1039/B805407J](https://doi.org/10.1039/B805407J)
4. Earl, J.S.; Wood, D.J.; Milne, S. J.; *J. Phys: Conference Series*, **2006**, *26*, 268.
DOI: [10.1088/1742-6596/26/1/064](https://doi.org/10.1088/1742-6596/26/1/064)
5. Aoki, H.; Japanese Association of Apatite Science, *Tokyo, Japan*, **1991**, 179.
6. Legeros, R.Z.; Myers, H., Ed.; Karger: *Basel, Switzerland*, **1991**, *15*, 109.
7. Ashley, B.; *Current Orthopaedics*, **2007**, *21*, 280.
DOI: [10.1016/j.cuor.2007.06.005](https://doi.org/10.1016/j.cuor.2007.06.005)
8. Pamela, H.; Klaas G. De.; *Journal of Tissue Engineering and Regenerative Medicine*, **2007**, *1*, 25.
DOI: [10.1002/term.5](https://doi.org/10.1002/term.5)


9. Taniguchi, M.; Takeyema, H.; Mizunna, I.; Shinagawa, N.; Yura, J.; Yoshikawa, N.; Aoki, H.; *Japan Journal of Artificial Organs*, **1991**, 20, 460.
10. Silva, R.V.; Bertran, J.A.; Moreira, N.H.; *International Journal of Oral and Maxillofacial Surgery*, **2005**, 34, 178.
DOI: [10.1016/j.ijom.2004.06.005](https://doi.org/10.1016/j.ijom.2004.06.005)
11. Kenneth, S.V.; Xing, Z.; Jennifer, B.M.; Mark, W.; Choll, W.K.; *Acta Biomaterialia*, **2007**, 3, 910.
DOI: [10.1016/j.actbio.2007.06.003](https://doi.org/10.1016/j.actbio.2007.06.003)
12. Poinern, G.E.; Brundavanam, R.K.; Mondinos, N.; Jiang, Z.; *Ultrasonics Sonochemistry*, **2009**, 16, 469.
DOI: [10.1016/j.ultsonch.2009.01.007](https://doi.org/10.1016/j.ultsonch.2009.01.007)
13. Gopi, D.; Indira, J.; Collins, V.; Prakash, A.; Kavitha, L.; *Spectrochimica Acta Part A*, **2009**, 74, 282.
DOI: [10.1016/j.saa.2009.05.021](https://doi.org/10.1016/j.saa.2009.05.021)
14. Ali Poursamar, S.; Azami, M.; Mozafari, M.; *Colloids and Surfaces B: Biointerfaces*, **2011**, 84, 310.
DOI: [10.1016/j.colsurfb.2011.01.015](https://doi.org/10.1016/j.colsurfb.2011.01.015)
15. Wang, Y.Z.; Fu, Y.; *Mater. Lett.*, **2011**, 65, 3388.
DOI: [10.1016/j.matlet.2011.07.095](https://doi.org/10.1016/j.matlet.2011.07.095)
16. Nasiri-Tabrizi, B.; Honarmandi, P.; Ebrahimi-Kahrizsangi, R.; Honarmandi, P.; *Mater. Lett.*, **2009**, 63, 543.
DOI: [10.1016/j.matlet.2008.11.030](https://doi.org/10.1016/j.matlet.2008.11.030)
17. Padmanabhan, S.K.; Balakrishnan, A.; Chu, M.C.; Lee, Y.J.; Kim, T.N.; Cho, S.J.; *Particuology*, **2009**, 7, 466.
DOI: [10.1016/j.partic.2009.06.008](https://doi.org/10.1016/j.partic.2009.06.008)
18. Koumoulidis, G.C.; Katsoulidis, A.P.; Ladavos, A.K.; Pomonis, P.J.; Trapalis, C.C.; Sdoukos, A.T.; Vaimakis, T.C.; *J. Colloid Interface Sci.* **2003**, 259, 254.
DOI: [10.1016/S0021-9797\(02\)00233-3](https://doi.org/10.1016/S0021-9797(02)00233-3)
19. Salgado, A.J.; Coutinho, O.P.; Reis, R.L.; *Macromol Biosci.* **2004**, 4, 743.
DOI: [10.1002/mabi.200400026](https://doi.org/10.1002/mabi.200400026)
20. Jagadale, P.N.; Kulal, S.R.; Joshi, M.G.; Jagtap, P.P.; Khetre, S.M.; Bamane, S.R.; *Materials Science-Poland*, **2013**, 31, 269.
DOI: [10.274 8/s 13536-012-0099-8](https://doi.org/10.274 8/s 13536-012-0099-8)
21. Gajbhiye, N.S.; Bhattacharyya, U.; Darshane, V.S.; *Thermochim Acta*, **1995**, 264, 219.
DOI: [10.1016/0040-6031\(95\)02331-U](https://doi.org/10.1016/0040-6031(95)02331-U)
22. Sun, Y.; Yang, H.; Tao, D.; *Ceram. Int.* **2011**, 37, 2917.
DOI: [10.1016/j.ceramint.2011.03.030](https://doi.org/10.1016/j.ceramint.2011.03.030)
23. Kulal, S.R.; Khetre, S.S.; Jagadale, P.N.; Gurme, V.M.; Waghmode, D.P.; Kolekar, G.B. Sabale, S.R.; Bamane, S. R.; *Mater. Lett.*, **2012**, 84, 169.
DOI: [10.1016/j.matlet.2012.06.025](https://doi.org/10.1016/j.matlet.2012.06.025)
24. Cullity, B.D.; *Addison-Wesley, London*, **1956**, 99.
25. Singh, O.P.; Muhunthan, N.; Singh, V.N.; Singh, B.P.; *Adv. Mater. Lett.*, **2015**, 6, 2.
DOI: [10.5185/amlett.2015.6584](https://doi.org/10.5185/amlett.2015.6584)
26. Gopi, D.; Nithiya, S.; Shinyjoy, E.; Kavitha, L.; *Spectrochimica Acta Part A*, **2012**, 92, 194.
DOI: [10.1016/j.saa.2012.02.069](https://doi.org/10.1016/j.saa.2012.02.069)
27. Stanic, V.; Janackovic, D.; Dimitrijevic, S.; Tanaskovic, S.B.; Mitric, M.; Pavlovic, M.S.; Krstic, A.; Jovanovic, D.; Raicevic, S.; *Applied Surface Science*, **2011**, 257, 4510.
DOI: [10.1016/j.apsusc.2010.12.113](https://doi.org/10.1016/j.apsusc.2010.12.113)
28. Lee, E.J.; Koh, Y.H.; Yoon, B.H.; Kim, H.E.; Kim, H.W.; *Mater. Lett.*, **2007**, 61, 2270.
DOI: [10.1016/j.matlet.2006.08.065](https://doi.org/10.1016/j.matlet.2006.08.065)
29. Mansur, A.A.P.; Mansur, H.S.; *Mater. Sci. and Eng. C*, **2010**, 30, 288.
DOI: [10.1016/j.msec.2009.11.004](https://doi.org/10.1016/j.msec.2009.11.004)
30. Chen, J.P.; Chang, Y.S.; *Colloids and Surfaces B: Biointerfaces*, **2011**, 86, 169.
DOI: [10.1016/j.colsurfb.2011.03.038](https://doi.org/10.1016/j.colsurfb.2011.03.038)
31. Ramay, H.R.; Zhang, M.; *Biomaterials*, **2003**, 24, 3293.
DOI: [10.1016/S0142-9612\(03\)00171-6](https://doi.org/10.1016/S0142-9612(03)00171-6)

Advanced Materials Letters

Copyright © 2016 VBRI Press AB, Sweden
www.vbripress.com/aml

Publish your article in this journal

Advanced Materials Letters is an official international journal of International Association of Advanced Materials (IAAM, www.iaamonline.org) published monthly by VBRI Press AB from Sweden. The journal is intended to provide high-quality peer-review articles in the fascinating field of materials science and technology particularly in the area of structure, synthesis and processing, characterisation, advanced-state properties and applications of materials. All published articles are indexed in various databases and are available download for free. The manuscript management system is completely electronic and has fast and fair peer-review process. The journal includes review article, research article, notes, letter to editor and short communications.



VBRI Press
a rapid publication platform

A
Monthly
Journal

